

1 **A central place foraging seabird flies at right angles to the wind to jointly**
2 **optimize locomotor and olfactory search efficiency**

3 Francesco Ventura^{1*}, Paulo Catry², Maria P. Dias³, Greg A. Breed⁴, Arnau Folch⁵, José Pedro
4 Granadeiro¹

5 ¹CESAM, Departamento de Biologia Animal, Faculdade de Ciências, Universidade de
6 Lisboa, Campo Grande, 1749-016 Lisboa, Portugal, www.cesam.ua.pt

7 ²MARE – Marine and Environmental Sciences Centre, Ispa – Instituto Universitário, Rua
8 Jardim do Tabaco 34, 1149-041 Lisboa, Portugal, www.mare.ispa.pt

9 ³Centre for Ecology, Evolution and Environmental Changes (cE3c), Faculdade de Ciências
10 da Universidade de Lisboa, Portugal. ORCID: 0000-0002-7281-4391

11 ⁴Institute of Arctic Biology, University of Alaska, Fairbanks, Fairbanks, Alaska, USA;
12 uaf.edu/iab/

13 ⁵Geociencias Barcelona – Consejo Superior Investigaciones Cientificas (GEO3BCN-CSIC),
14 Barcelona, Spain

15

16 *Corresponding author: Francesco Ventura

17 Email: fraventura.92@gmail.com

18 **Abstract**

19 To increase the probability of detecting odour plumes, and so increase prey capture
20 success, when winds are stable central place foraging seabirds should fly crosswind to
21 maximize the round-trip distance covered. At present, however, there is no empirical
22 evidence of this theoretical prediction. Here, using an extensive GPS tracking dataset, we
23 investigate, for the first time, the foraging movements of Bulwer's petrels (*Bulweria*
24 *bulwerii*) in the persistent North Atlantic trade winds. To test the hypotheses that in stable
25 winds petrels use crosswind to maximize both the distance covered and the probability of
26 detecting olfactory cues, we combine state-space models, generalized additive models and
27 Gaussian plume models. Bulwer's petrels had the highest degree of selectivity for
28 crosswinds documented to date, often leading to systematic zig-zag flights. Crosswinds
29 maximized both the distance travelled and the probability of detecting odor plumes
30 integrated across the round-trip (rather than at any given point along the route, which
31 would result in energetically costly return flight). This evidence suggests that petrels plan
32 round-trip flights at departure, integrating expected costs of homeward journeys. Our
33 findings, likely true for other seabirds in similar settings, further highlight the critical role
34 of wind in seabird foraging ecology.

35

36 **Keywords**

37 Bulwer's petrel; central place foraging; flight behaviour; olfaction; wind; zig-zag

38 1. Background

39 Animals should minimize the energetic costs of movement during foraging while
40 maximizing caloric intake to maximize net energetic gain [1–3]. Foraging strategies that
41 maximize net energy intake take many forms depending upon a species' ecological niche
42 and physiological and morphological adaptations. One very common constraint to bouts
43 of foraging is found in species that must return to a "central place", usually to provide
44 care for altricial progeny left at a rookery, nest, or den. Such species make foraging trips
45 that last from a few minutes to a few days, but must return to the site from which the
46 foraging trip originated [4].

47 The foraging movements during breeding of seabirds are made from central places. This
48 includes species from the order Procellariiformes (tube-nosed seabirds; the albatrosses,
49 petrels, and shearwaters). Members of this order spend most of their lives on the wing in
50 the open ocean, returning to land only a few months per year to breed [5]. During
51 breeding seasons, despite the constraint of a central place, foraging trips of seabirds can
52 still cover thousands of kilometers [6]. This striking motility is underpinned by an
53 exceptionally efficient flight strategy known as "dynamic soaring", whereby seabirds
54 exploit the wind velocity gradients ("wind-shear") close to the surface of the ocean,
55 ascending into the wind and descending with the wind, thus gleaning aerodynamic
56 kinetic energy [7–11]. Furthermore, while wind–shear soaring provides most (~80–90%) of
57 the total energy for sustained soaring [8], additional energy can be extracted by seabirds
58 by exploiting wave-induced features of the wind fields and localised updrafts produced
59 by wind blowing over waves [8]. When carrying out the swooping manoeuvres
60 characteristic of dynamic soaring [12], seabirds exhibit a movement orientation bias
61 relative to wind direction ("anemotaxis"), typically using crosswinds (i.e. blowing
62 perpendicularly to the bird heading) and quartering-tailwinds (i.e. blowing from behind,
63 at an acute angle to the bird direction of movement) [11] to maximize their traveling speed
64 [9,13,14] and minimize their energy expenditure [9,15].

65 Wind direction and intensity greatly impact advective odor dispersal, shaping the odor
66 landscape on the surface of the ocean [16,17]. Many procellariiform seabirds use their
67 highly developed sense of smell to locate widely distributed food patches across long
68 distance foraging flights [16,17] as well as to identify partners and nests [18]. In fact,
69 Procellariiformes have among the largest olfactory bulbs of birds [19]. This is particularly
70 true for nocturnal seabirds, which have a relatively larger olfactory bulb size than diurnal
71 species [20]. To inform olfactory foraging, seabirds use anemotactic flight strategies [16].
72 For instance, when searching for food, wandering albatrosses (*Diomedea exulans*) flew
73 using crosswinds and quartering-tailwinds to maximize the probability of crossing an
74 odor plume, and are able to detect odor sources at ranges of up to 20 km [17]. Evidence of
75 crosswind odor plume search strategies have been documented in other taxa, such as
76 insects [21,22].

77 The effect of wind on the costs of movement of central place foraging seabirds has been
78 widely investigated from both theoretical [23] and empirical [e.g. 6,9,12] perspectives.

79 Based on theoretical models, crosswind flight is predicted to be the optimal anemotactic
80 strategy in a wind field that remains constant over the spatial and temporal domain of use
81 [23]. These theoretical predictions are fairly intuitive, because birds flying with the
82 assistance of advantageous tail winds during the outward section of the flight would have
83 to face the costs of returning to the colony with headwinds. Due to the longer duration of
84 the headwind homeward flight and the extra food load, the costs would exceed the
85 benefits, making this strategy less profitable than crosswind flight [23].

86 Thus, in stable and uniform winds, crosswind flight is predicted to be the most
87 advantageous anemotactic strategy for seabirds to both minimize the energetic flight costs
88 of combined outbound and inbound segments of foraging trips from central places, while
89 also maximizing the number of odor plumes crossed for a given distance travelled. At
90 present, no empirical observations have provided full support for these theoretical
91 predictions and, in fact, for the reasons outlined below, key deviations from these
92 predictions have instead been observed in other systems.

93 Historically, the geographical coverage of seabird tracking studies has been biased toward
94 high latitude regions, which are characterized by much more variable wind conditions. In
95 such conditions, instead of using crosswind, seabirds can carry out fast, long looping
96 routes orienting at the most favorable angle with respect to the local wind conditions
97 throughout the foraging trip [e.g. 9]. Use of wind fields by seabirds living in tropical and
98 subtropical latitudes, where predictable trade winds prevail [24], is less well understood
99 [25]. Tracking studies have also historically tended to focus on large seabirds able to carry
100 heavy early generation tracking devices [24]. These large species are typically diurnal, feed
101 on epipelagic prey, and show some levels of foraging site fidelity to productive areas
102 associated with seamounts, shelf breaks, upwelling regions, and frontal zones [26–29]. In
103 these situations, advantages of commuting to these areas may outweigh the sub-optimal
104 energetic subsidies available during the commute from central places [9,13]. Furthermore,
105 upon reaching productive areas, seabirds may engage in area-restricted-searches (ARS),
106 performing slower and more tortuous movement bursts [16]. During ARS, birds may
107 deviate from a crosswind flight strategy by pursuing visual cues regardless of the wind
108 conditions experienced, for instance, by directing their flight towards other foraging
109 seabirds [30], fish schools, or fishing vessels [31,32]. Considerably less is known about the
110 foraging ecology of smaller nocturnal seabirds feeding on mesopelagic prey. These birds
111 may rely on visual cues to a limited extent, feed opportunistically *en route* on less
112 predictable food resources (such as vertically migrating prey present near the ocean
113 surface mostly at night) and do not forage in large aggregations. These features suggest
114 that they should maximally benefit from crosswind flight to facilitate olfactory food
115 search.

116 Here, for the first time, we analyze the flight behavior and use of wind by Bulwer's petrel
117 (*Bulweria bulwerii*), a ca. 100-g nocturnal [33,34] specialist predator of mesopelagic prey
118 [35] foraging in the persistent North Atlantic trade winds. The ecological features of this
119 study system make it particularly well-suited for investigating the role of wind in shaping

120 the movement patterns of petrels and other similar seabirds. Recent work using
121 geolocation devices found that breeding Bulwer's petrels use waters both within and
122 beyond the northern boundary of the trade winds belt [33]. This feature thus provides
123 enough environmental contrast to test if individuals adjust their flight strategy depending
124 on whether their central place foraging trips are performed only in predictable trade
125 winds or if their strategy changes when trips move beyond the trade winds belt and into
126 less predictable wind fields. Specifically, we assessed support for the following
127 hypotheses:

128 H1) Birds performing central place foraging trips in persistent and predictable wind fields
129 carry out trips orienting at 90° (orthogonally) to the prevailing trade winds. We predict
130 that this preference for crosswind flights would allow birds to maximize the distance
131 covered per unit time and minimize the energetic costs of round-trip locomotion. We also
132 predict that, when birds use areas characterized by a higher variability in wind conditions,
133 they would sustain their trips exploiting more assistance from the wind (i.e. a higher tail
134 wind component), when available.

135 H2) Birds performing crosswind flights maximize olfactory search information by
136 optimizing the probability of detecting odor plumes. We predict that birds exploiting
137 olfactory cues throughout their flight would consistently show a preference for crosswinds
138 both during day time (when visual cues can be used more extensively) and darkness
139 (when visual cues are limited or absent). Flying perpendicular to prevailing winds should
140 maximize the distance at which a source can be detected and the overall area scanned
141 using olfaction along the route.

142

143 **2. Methods**

144 **2.1 Data collection**

145 We deployed GPS loggers on incubating Bulwer's petrels from colonies at Deserta Grande
146 and Selvagem Grande (Madeira, Portugal) during three breeding seasons (June-July of
147 2015, 2016 and 2021). We used Pathtrack (<https://www.pathtrack.co.uk>) nanoFix-GEO
148 GPS-loggers (weight of 2.3g), corresponding to ca. 2.3% of adult petrels body mass. Tags
149 were programmed to record locations on two schedules. In the first, loggers recorded
150 points every hour, which allowed for analysis of flight throughout the entire foraging trips
151 from the moment of departure to return and distinguish between "nearby" and "distant"
152 trips. In the second, loggers recorded locations every 3 minutes for six hours each day,
153 which allowed us to investigate wind use at a high resolution and with minimal chance of
154 missed state-changes. Prior to analysis, all the tracks were linearly interpolated using the
155 package adehabitatLT [36] in R software [37] to impute missing data. The extent of
156 interpolation was minimal (less than 2% of the points were imputed) (electronic
157 supplementary material S1).

158 The wind raster files were downloaded from the ECMWF ERA-5 database
159 (<https://cds.climate.copernicus.eu/cdsapp>), at a spatial resolution of 0.25° and temporal
160 resolution of 1 hour. The following variables were calculated for each GPS relocation:
161 wind direction (in degrees), wind intensity (ms^{-1}), tail wind component (hereafter "TWC",
162 calculated as in [38]), and wind direction relative to the bird bearing (hereafter ' Δ angle',
163 calculated as in [13]). Δ angle ranged from a minimum of 0° (tail winds, aligned with the
164 direction of movement) to a maximum of 180° (head winds, blowing in the opposite
165 direction of movement).

166 **2.2 Movement analysis**

167 We fit discrete-time hidden-Markov-models (HMMs) using the R package `momentuHMM`
168 [39] to classify the behavioral states of the petrels along the tracks, separately for the 1 h
169 and the 3-min datasets. To improve movement behaviour classification, we accounted for
170 the intrinsic effect of TWC on the mean parameter of the step length distribution, for both
171 the travelling and searching states (electronic supplementary material S2). To decode the
172 sequence of behavioural states of the Markov chain most likely to have produced the
173 observed data given the fitted HMM, we used the Viterbi algorithm [40]. We assumed that,
174 along the 1 h resolution tracks, the petrels were in one of two behavioral states: "transit", in
175 which the underlying drive is to move at high speed in a persistent heading; or "search", in
176 which the drive is to search for food upon entering a foraging patch [41]. In the 3-min
177 resolution tracks, we assumed that the petrels were in one of these three states: "in flight",
178 when the birds spent the entire move step flying; "on water", when the animals spent the
179 entire move step sitting on the water surface to ingest and process food or rest; and
180 "mixed", an intermediate state in which the animals spent part of the step in flight and part
181 on the water, indicative of foraging attempts (electronic supplementary material S2).

182 **2.3 Wind use analysis**

183 The distribution of Δ angle for the different states in the 3-min and 1 h resolution tracks
184 was calculated, quantifying separate Δ angle distributions for points recorded during day
185 and night. The analysis subsequently evaluated the effect of wind on ground speed of the
186 petrels. For this part of the analysis, we used only segments of the 1 h resolution tracks
187 that were classified by the HMM as "transit". When birds were in this state, we assumed
188 that the relationship between the wind and ground speed was only minimally affected by
189 other activities, such as searching for food or resting. We fit generalized additive mixed
190 effect models (GAMMs, hereafter referred to simply as "wind model") with the `mgcv`
191 package [42] in R to quantify the effect of Δ angle, wind intensity and their interaction on
192 the ground speed attained by transiting petrels along the 1-h resolution tracks. The best set
193 of candidate variables to retain in the GAMM was selected based on AIC [43] (electronic
194 supplementary material S3).

195 **2.4 Odor plume model**

196 The objective of this analysis was to evaluate how the effective area searched using
197 olfaction is affected by the Δ angle of flight relative to wind direction and wind intensity. It

198 is important to highlight that, in this analysis, we do not consider the spatial location of
199 the odour source (i.e. the prey). Rather, the objectives of the analysis are the following:
200 first, to estimate the theoretical instantaneous range at which prey can be detected using
201 olfaction (i.e. the "olfactory bandwidth", see below) by birds flying under a range of
202 Δ angle and wind intensity values; second, to evaluate how the theoretical area scanned
203 using olfaction by birds is affected by the predicted "olfactory bandwidth" and ground
204 speed attained in given Δ angle and wind intensity values. To do this, we built theoretical
205 Gaussian plume models [44] (hereafter referred to as "odor plume models") to analytically
206 describe the wind-driven advection of odor plumes. We developed the odor plume model
207 with constant emission rate from a source on the water surface, diffusivities along the y-
208 and z-axis of $1000 \text{ m}^2\text{s}^{-1}$, constant decay and advection with the flow of a constant and
209 uniform wind. Under these parameters, the theoretical odor plume models were used to
210 quantify the concentration of odor molecules in every cell (with resolution of 5 m^2) of a 20
211 km^2 grid, as a function of wind intensity and distance (on the x- and y-axis) from the odor
212 source. We assumed that the birds could detect smell when it decayed to $2 \cdot 10^{-4}$ of the
213 concentration measured at a distance of 1 m from the source. This choice yielded oval
214 contour lines where the smell was detectable up to a maximum distance from source of
215 approximately 5 km, which is consistent with the detection distance documented in
216 albatrosses [17]. A set of odor plume models and resulting oval smell detection contour
217 lines were generated with wind intensities ranging from 1 to 15 ms^{-1} . Then, integrating the
218 results from the odor plume model with the predictions from the wind model (i.e. the
219 predicted ground speed attained at a given Δ angle and wind intensity), we calculated two
220 key quantities. First, we calculated the theoretical "olfactory bandwidth", i.e. the maximum
221 distance from the source at which the birds are predicted to detect the prey smell, for each
222 value of Δ angle and wind intensity, calculated applying trigonometric formulae (fig. 1).
223 Second, we calculated the theoretical area (km^2) scanned by olfaction by a bird flying at a
224 given Δ angle and wind intensity during one movement step (1-hour), calculated by
225 multiplying the olfactory bandwidth by the predicted distance covered (electronic
226 supplementary material S3). A sensitivity analysis was carried out, which showed that the
227 results obtained on the effects of Δ angle and wind intensity on the area scanned are robust
228 to the parameter specification (electronic supplementary material S3).

229 **2.5 Track simulation: distance covered and area scanned**

230 We applied a simulation framework to investigate whether, along the realized trips, birds:
231 1) maximize their speed; and 2) maximize the area scanned using olfaction along their
232 entire round-trip foraging route from a central place. In short, a set of "random" and
233 "rotated" simulated tracks were designed, which were equivalent (i.e. covering the same
234 distance) to their corresponding real tracks, but along these simulated routes the birds
235 travelled at a different Δ angle. We compared the duration and the area olfactorily scanned
236 along the simulated trips to the duration and area scanned throughout the real trips
237 (electronic supplementary material S4).

238

239 **3. Results**240 **3.1 Movement analysis**

241 Bulwer's petrels exhibited a large foraging range during breeding (see [45] for a
 242 comparison on other breeding Procellariiformes foraging ranges). Two high-usage areas
 243 were identified: a "nearby" area, located off the coasts of the Canary islands and West
 244 Africa, within the trade winds belt; a "distant" area, encompassing the waters to the
 245 northern edge of the trade winds belt and beyond, to the north of Azores, reached by the
 246 birds through clockwise looping trips (fig. ESM1 in the electronic supplementary
 247 material). The tracks showed a high degree of movement directionality. The birds mostly
 248 flew at constant heading between few sharp turning points, resulting in a series of zig-
 249 zagging trajectories. This is evident both in the 1-h resolution tracks (particularly off the
 250 coasts of the Canaries and West Africa, but also near the coasts of the Azores) and in the 3-
 251 min resolution tracks (fig. 2), in which the petrels often did not change heading during the
 252 whole duration of the 6 hour segments. On average, the complete 1-h resolution foraging
 253 trips of Bulwer's petrels ($n = 18$ complete tracks) lasted 11.5 days (s.d. 1.8 days). The
 254 average total distance travelled was 4143.6 km (s.d. 981.5 km) and the average maximum
 255 distance from the colony was 1137.9 km (s.d. 605.1 km). The maximum distance from the
 256 colony was not significantly correlated with the temporal duration of the trips (Pearson's
 257 correlation, $r_{16} = -0.04$, $p = 0.89$). An average of 52% (s.d. = 18%) of the relocations were
 258 classified as searching. Overall, both the sections of the tracks classified as transit and
 259 search were characterized by a high degree of movement directionality. Specifically, the
 260 mean turning angle was equal to -0.4° (circular standard deviation = 30.8°) for the transit
 261 state and -1.4° (circular standard deviation = 76.3°) for the search state. The average speed
 262 during transit was 22.2 kmh^{-1} (s.d. = 5.5 kmh^{-1}) whereas birds in the search state flew at an
 263 average speed of 9.06 kmh^{-1} (s.d. = 6.1 kmh^{-1}). Along the 3-min resolution tracks (fig. 2) the
 264 average ground speed was equal to: 26.4 kmh^{-1} (s.d. 7.2 kmh^{-1}) when birds were in flight;
 265 3.1 kmh^{-1} (s.d. 3.5 kmh^{-1}) when they were on the water; and 19.5 kmh^{-1} (s.d. 5.5 kmh^{-1})
 266 when they were in the "mixed" state. The 3-min resolution tracks also showed high
 267 movement directionality. Specifically, the turning angle of the birds was equal to 0.1°
 268 (circular standard deviation = 20.8°) when in flight; -0.4° (circular standard deviation =
 269 70.5°) when the birds were sitting on the water; and 0.5° (circular standard deviation =
 270 28.9°) when the birds were in the "mixed" state.

271 **3.2 Wind use analysis**

272 The petrels exhibited an extreme degree of selectivity for crosswinds (table 1 and fig. 3).
 273 This was evident both during the "in flight" and the "mixed" sections of the 3-min
 274 resolution tracks, but also along the "transit" and "search" sections of the 1-h resolution
 275 trips, resulting in strikingly narrow Δ angle density curves, particularly compared to the
 276 wind use of other procellariiform seabirds in the region (fig. 3b). When "in flight" along the
 277 64 tracked flight bouts at 3-min resolution, petrels mostly flew orienting almost perfectly
 278 orthogonally with respect to the wind (median Δ angle = 89.9°), spending 64% of their "in
 279 flight" time flying at Δ angle between 70° and 110° . Similarly, when in the "mixed" state,

280 they used crosswinds, flying at a median Δ angle of 85.9° (table 1 and fig. 3a). The wind use
 281 along the 1-h resolution tracks (comprising a total of 22 trips, of which 9 "nearby" and 13
 282 "distant") is largely consistent with the findings described above (particularly so for the
 283 "nearby" trips). The petrels showed a preference for crosswind flight, both during the
 284 transit and the search state (table 1 and fig. 3b). The Δ angle used by the birds along the
 285 "nearby" and "distant" 1-h resolution trips was significantly different (Mann-Whitney-
 286 Wilcoxon Test, $p < 0.001$). The petrels had a higher selectivity for crosswind along the
 287 nearby trips, whereas their wind use shifted towards more quartering-tailwinds during
 288 the distant trips (table 1). Moreover, the TWC experienced along the nearby and distant
 289 trips was significantly different (Mann-Whitney-Wilcoxon Test, $p < 0.001$); specifically,
 290 along the distant trips the birds travelled with a stronger support from the wind (median
 291 TWC = 1.9 kmh^{-1} ; interquartile range= $0.1\text{--}3.7 \text{ kmh}^{-1}$) compared to the nearby tracks
 292 (median TWC = 0.2 kmh^{-1} ; interquartile range= $-1.9\text{--}1.8 \text{ kmh}^{-1}$). Overall, the birds
 293 consistently used crosswinds along the 3-min resolution tracks, both during day and night
 294 (table 1), resulting in Δ angle values not significantly different (Mann-Whitney-Wilcoxon
 295 Test, $p = 0.51$). This result was also true for the 1-h resolution tracks (Mann-Whitney-
 296 Wilcoxon Test, $p = 0.54$) (table 1).

297 The results of the wind model based on the locations classified as "transit" showed that, at
 298 each movement step, the petrels are predicted to attain highest ground speed with
 299 favorable tail to quartering-tailwinds. Specifically, the wind model retained Δ angle, wind
 300 intensity and their interaction as significant predictors of ground speed. The ground speed
 301 was non-linearly affected by Δ angle and wind intensity, with a maximum speed attained
 302 by the birds at values of Δ angle $\approx 30^\circ$, particularly when traveling with stronger winds
 303 (fig. 4a). The results of a wind model fitted to the 3-min resolution tracks are largely
 304 consistent (electronic supplementary material S3).

305 **3.3 Odor plume model**

306 For all wind intensities, the olfactory bandwidth ("C2" in fig. 1) is maximum for Δ angle
 307 values of 90° (fig. ESM4 in electronic supplementary material). At low wind intensities,
 308 when the predicted effect of wind on the ground speed of the petrels is minimal, a Δ angle
 309 of 90° maximizes the area scanned (km^2 in 1-h) by the olfactory searching birds (fig. 4b). As
 310 the wind intensity increases, the oval smell detection contour becomes stretched along the
 311 direction of wind flow (fig. ESM3 in electronic supplementary material). Furthermore, for
 312 increasing wind intensities, the birds are predicted to attain higher speeds with favorable
 313 tail to quartering-tailwinds, whereas the use of crosswinds results in lower speeds. In turn,
 314 at intermediate (e.g. 7 ms^{-1} , which is the average wind intensity experienced by the petrels
 315 along the 1-h resolution tracks) and high (e.g. 15 ms^{-1}) wind intensities, the peak of the
 316 theoretical area scanned shifts towards Δ angle values $< 90^\circ$ (between 60° and 65° , fig. 4b).

317 **3.4 Track simulation: distance covered and area scanned**

318 The real tracks realized by the transiting petrels were significantly faster than the random
 319 (paired t-test, $t = -5.03$, d.f. = 17, $p < 0.001$) and rotated trips (paired t-test, $t = -3.66$, d.f. =

320 17, $p = 0.002$). The real duration was, on average, 175 h and 211 h (i.e. 136% and 164%)
 321 faster than the duration of the respective random and rotated trips. The area scanned
 322 throughout the real trips was also significantly wider than the area scanned along the
 323 random (paired t-test, $t = 3.11$, d.f. = 17, $p = 0.006$) and rotated (paired t-test, $t = 7.35$, d.f. =
 324 17, $p < 0.001$) tracks. More specifically, the area scanned along the real trips was on average
 325 646 km² and 1304 km² (i.e. 5% and 11%) wider than the area scanned along the respective
 326 random and rotated trips (fig. ESM6 in electronic supplementary material).

327

328 **4. Discussion**

329 Bulwer's petrels have a higher degree of selectivity for crosswinds than any other seabird
 330 tracked to date. This strategy, exhibited both when in transit and searching, and consistent
 331 across different observation resolutions of our tracking dataset, is striking if compared to
 332 the wind use of other procellariiform seabird populations from the same region (fig. 3b
 333 and electronic supplementary material S2). Our results show that crosswind flight enables
 334 the birds to maximize both the distance covered and the area olfactorily scanned
 335 throughout their trips. Furthermore, for the first time, we document an emerging property
 336 (discussed below) of the central place foraging trips of the petrels, underpinned by the
 337 high selectivity for crosswinds: a systematic zig-zag flight, both during the transit and the
 338 search sections of their tracks.

339 **4.1 Crosswind flight to maximize distance covered in stable winds**

340 Our results provide strong empirical support for the hypothesis that crosswind flight
 341 allows petrels to maximize the distance covered throughout their central place foraging
 342 routes (H1). Bulwer's petrels are predators of mesopelagic prey [35] and do not
 343 consistently target predictably rich foraging hotspots [33]. Rather, they forage over deep
 344 oceanic waters on unpredictable prey at coarse (1–100 km²) and meso scales (100–1000
 345 km²), covering as much distance as possible to maximize the probability of
 346 opportunistically finding prey along their routes.

347 Here we clearly show that crosswind does not maximize the ground speed along each
 348 movement step. As predicted by the wind model, birds fly the fastest with quartering-
 349 tailwinds, which aligns with the findings on the speed and energy expenses of other
 350 dynamic soaring seabirds, such as albatrosses and gadfly petrels [6,9,15]. Rather than
 351 representing a strategy to maximize their instantaneous speed, Bulwer's petrels use
 352 crosswinds to maximize the distance covered along their entire round trips from central
 353 places carried out in predictably stable wind fields. This anemotactic strategy is different
 354 than, for instance, that of gadfly petrels (e.g. Desertas petrels, *Pterodroma deserta*), which
 355 design fast long tracks consistently selecting a wind Δ angle that enable them to maximize
 356 their instantaneous speed [6]. Compared to the larger gadfly petrels, Bulwer's petrels are
 357 smaller, fly at a lower ground speed and have lower wing loading and aspect ratio [14].
 358 These anatomical features make headwind flight particularly disadvantageous [14] and
 359 potentially unsustainable and, in fact, the petrels only rarely engaged in headwind flight.

360 Tracked petrels also travelled beyond the trade winds belt, carrying out long clock-wise
 361 routes. Rather than commuting to distant foraging hotspots, we argue that the benefit of
 362 such longer trips may be the greater distance covered to increase the probability of
 363 encountering food en route. In line with previous evidence [33], we found that the
 364 Bulwer's petrel foraging range was not correlated with the temporal duration of their
 365 journeys owing to the higher average speed along the distant trips than along the near
 366 trips, underpinned by the use of comparably more advantageous wind Δ angles. By
 367 exploiting higher variability in winds, petrels consistently chose more favorable Δ angles
 368 and received more assistance from the wind (i.e. higher TWC) along the distant trips,
 369 resulting in the longer commutes being significantly faster than the respective simulated
 370 trajectories.

371 All these findings strongly suggest that Bulwer's petrels rely on an impressive knowledge
 372 of the regional wind availability and real time wind fields. When birds stay within the
 373 stable and more predictable trade winds region, they use crosswinds to cover as much
 374 distance as possible along the entire route, a strategy that will prevent them from
 375 performing long headwind commutes on the way back. Such selection for integrated
 376 optimization over the course of multi-day return route from a central place suggests that,
 377 upon departure, these animals may plan their overall route across that entire period, and
 378 anticipate the expected winds that they will experience days later when they return to the
 379 colony.

380 **Crosswind flight and area scanned by olfaction**

381 In line with previous evidence [17], we found that crosswind flight enables the birds to
 382 maximize the olfactory bandwidth, supporting H2. In fact, at low wind intensities,
 383 crosswind flight (i.e. Δ angle values $\sim 90^\circ$) maximized both the olfactory bandwidth and
 384 the theoretical area scanned. However, for higher wind intensities, the use of quartering-
 385 tailwinds results in a gain in speed and therefore in the area scanned per unit time that
 386 offsets the loss incurred from the smaller instantaneous range of detection of odour
 387 plumes (compared to the larger olfactory bandwidth achievable with crosswind). Our
 388 model highlights that the result of this trade-off varies with wind speed, but under most
 389 conditions faced by the petrels (the typical wind intensity in the study area is $\sim 7 \text{ ms}^{-1}$), the
 390 theoretical predictions on area scanned per unit time are qualitatively similar (greater
 391 overall area scanned for wind Δ angle smaller than 90° , between 60° and 65°). These values
 392 are smaller than the preferred Δ angle (ca. 90°) most intensely used by the petrels along
 393 their tracks. Yet, despite this discrepancy, the overall roundtrip trajectories realized by the
 394 birds allowed for a significantly larger area scanned using olfaction than their respective
 395 simulated ones. Hence, rather than maximizing the area scanned at any given point in the
 396 foraging trip, our results suggest that the extensive use of crosswinds enables these birds
 397 to maximize the area scanned along their entire central place foraging trip routes.

398 Our findings strongly support the hypothesis that Bulwer's petrels search for foraging
 399 opportunities using their sense of smell, both during day and night, relying on crosswind
 400 flight to detect olfactory cues and opportunistically find prey along their route. This may

401 be the key to the ecological success of many other small petrels with similar foraging
 402 ecologies, which have global distributions and some of the largest seabird populations on
 403 earth. We found that petrels are highly selective of crosswinds not only when realizing fast
 404 transit movements, but also when searching for food, consistently for the finer-scale and
 405 coarser resolution datasets. Moreover, the petrels exhibit a strikingly similar distribution
 406 of wind Δ angle both during day (when visual cues could be used more extensively) and
 407 night (when they are more visually limited). Had visual cues been used to detect prey, it
 408 would be reasonable to expect the foraging strategies and the movement behavior of
 409 petrels to differ considerably between night and day. Further evidence is also provided by
 410 the fine-scale movements documented in the 3-min tracks. In some sections, the birds
 411 seem to fly crosswind to detect odor plumes, track the smell upwind to the source upon
 412 detection, stop to forage, and then resume flying along the initial direction (fig. 5).

413 **Zig-zag**

414 An emerging property of the Bulwer's petrel tracks is a systematic crosswind zig-zag
 415 flight. This zig-zag flight occurs both at the large scale (1-h resolution), when the birds are
 416 carrying out fast transit movements, and at a smaller scale (3-min resolution), when they
 417 are performing ARS movements upon reaching areas offering good feeding opportunities
 418 (fig. 2). The 3-min dataset comprises large sections in which the petrels maintain constant
 419 heading, realizing straight crosswind tracks often for the whole duration of the recorded
 420 movement burst. Along some tracks, the birds performed sharp turns, changing heading
 421 by $\sim 180^\circ$ to fly in the direction from which they were coming. The extensive use of this
 422 crosswind zig-zag flight, and its potential importance as an efficient search strategy, is
 423 documented here for the first time.

424 Various anecdotal evidence from at-sea observations and both theoretical [8] and empirical
 425 studies [12] suggested that dynamic soaring albatrosses can fly without flapping their
 426 wings at virtually any angle with respect to the wind, including directly upwind, by
 427 "tacking" like a sail-boat. However, this implies several sections with an overall upwind
 428 heading and tacking manoeuvres with smaller turning angles compared to the sharp turns
 429 exhibited by the zig-zagging Bulwer's petrels. Furthermore, as we discussed above, the
 430 Bulwer's petrels very rarely engaged in upwind flight and are predicted to attain the
 431 lowest ground speed in such conditions. In fact, due to their wing morphology [14],
 432 sustained headwind flight may be particularly disadvantageous for Bulwer's and other
 433 small petrels. Hence, we argue that the systematic zig-zag undertaken by the petrels is
 434 underpinned by high selectivity for crosswind during the entire roundtrip, both to
 435 maximize the distance travelled and the area scanned olfactorily for foraging
 436 opportunities.

437 **Conclusion**

438 Under constant winds, Bulwer's petrels maximize the distance covered and the area
 439 scanned using olfaction by performing a systematic crosswind zig-zag flight. When
 440 conditions are suitable, petrels also undertake larger clock-wise looping routes, efficiently

441 designed to exploit the higher wind variability beyond the trade winds belt. The results of
442 this study provide novel elements shedding further light into adaptations of dynamic
443 soaring seabirds for the efficient use of stable and predictable winds. Such ecological
444 features make seabirds particularly sensitive to the effects of climate change on the ocean
445 winds. The general atmospheric circulation and particularly the intra-seasonal variability
446 in wind conditions in the subtropics are predicted to be highly impacted by climate
447 change [46,47]. In this context, a thorough understanding of the role played by wind in
448 movement ecology of seabirds is pivotal, with direct implications for conservation and
449 evidence-based management.

450

451 **Acknowledgments**

452 We are grateful to Teresa Catry, Isamberto Silva, Filipe Moniz, Miguel Lecoq, Martin Beal,
453 Joana Romero, Marie Claire Gatt, Maria Alho, Tegan Newman, Estefanía Pereira and the
454 wardens of Desertas and Selvagens Islands Nature Reserves for fieldwork support.
455 Instituto das Florestas e da Conservação da Natureza (and particularly Dília Menezes and
456 Carolina Santos) gave permissions and logistical support for the work. We are thankful to
457 Pedro Miranda for insightful discussions. We also thank two anonymous reviewers for
458 helpful comments on an earlier draft of this manuscript.

459

460 **Funding**

461 This work was funded by the Fundação para a Ciência e a Tecnologia (FCT, Portugal) and
462 the European Regional Development Fund through the projects: UIDB/04292/2020 and
463 UIDP/04292/2020, granted to MARE; UIDP/50017/2020, UIDB/50017/2020 and
464 LA/P/0094/2020, granted to CESAM; and PD/BD/135537/2018 awarded to FV.

465 **References**

- 466 1. Dickinson MH, Farley CT, Full RJ, Koehl MAR, Kram R, Lehman S. 2010 How animals
467 move : an integrative view. *Science (80)*. **288**, 100–106.
- 468 2. Nathan R, Getz WM, Revilla E, Holyoak M, Kadmon R, Saltz D, Smouse PE. 2008 A
469 movement ecology paradigm for unifying organismal movement research. *Proc. Natl. Acad.*
470 *Sci. U. S. A.* **105**, 19052–19059.
- 471 3. Krebs JR. 1978 Optimal foraging: decision rules for predators. In *Behavioural Ecology: An*
472 *Evolutionary Approach* (eds JR Krebs, NB Davies), pp. 23–63. Sutherland, MA.: Sinauer
473 Associates, Inc.
- 474 4. Hamilton III WJ, Watt KEF. 1970 Refuging. *Annu. Rev. Ecol. Syst.* **1**, 263–286.
- 475 5. Warham J. 1996 *The behaviour, population biology and physiology of the petrels*. Academic Press.
- 476 6. Ventura F, Granadeiro JP, Padget O, Catry P. 2020 Gadfly petrels use knowledge of the
477 windscape, not memorized foraging patches, to optimize foraging trips on ocean-wide
478 scales. *Proc. R. Soc. B Biol. Sci.* **287**, 20191775. (doi:10.1098/rspb.2019.1775)
- 479 7. Pennycuik CJ. 2002 Gust soaring as a basis for the flight of petrels and albatrosses
480 (Procellariiformes). *Avian Sci.* , 1–12.
- 481 8. Richardson PL. 2011 How do albatrosses fly around the world without flapping their
482 wings? *Prog. Oceanogr.* **88**, 46–58. (doi:10.1016/j.pocean.2010.08.001)
- 483 9. Weimerskirch H, Guionnet T, Martin J, Shaffer SA, Costa DP. 2000 Fast and fuel efficient?
484 Optimal use of wind by flying albatrosses. *Proc. R. Soc. B Biol. Sci.* **267**, 1869–1874.
485 (doi:10.1098/rspb.2000.1223)
- 486 10. Sachs G, Traugott J, Nesterova AP, Dell’Omo G, Kümme F, Heidrich W, Vyssotski AL,
487 Bonadonna F. 2012 Flying at no mechanical energy cost: disclosing the secret of wandering
488 albatrosses. *PLoS One* **7**. (doi:10.1371/journal.pone.0041449)
- 489 11. Kempton JA *et al.* 2022 Optimization of dynamic soaring in a flap-gliding seabird and its
490 impacts on large-scale distribution at sea. *Sci. Adv.*
- 491 12. Richardson PL, Wakefield ED, Phillips RA. 2018 Flight speed and performance of the
492 wandering albatross with respect to wind. *Mov. Ecol.* **6**, 1–15.
- 493 13. Wakefield ED, Phillips RA, Matthiopoulos J, Fukuda A, Higuchi H, Marshall GJ, Trathan
494 PN. 2009 Wind field and sex constrain the flight speeds of central-place foraging albatrosses.
495 *Ecol. Monogr.* **79**, 663–679.
- 496 14. Spear LB, Ainley DG. 1997 Flight behaviour of seabirds in relation to wind direction and
497 wing morphology. *Ibis (Lond. 1859)*. , 221–233.

- 498 15. Sakamoto KQ, Takahashi A, Iwata T, Yamamoto T, Yamamoto M, Trathan PN. 2013 Heart
499 rate and estimated energy expenditure of flapping and gliding in black-browed albatrosses.
500 *J. Exp. Biol.* **216**, 3175–3182. (doi:10.1242/jeb.079905)
- 501 16. Nevitt GA. 2008 Sensory ecology on the high seas: The odor world of the procellariiform
502 seabirds. *J. Exp. Biol.* **211**, 1706–1713. (doi:10.1242/jeb.015412)
- 503 17. Nevitt GA, Losekoot M, Weimerskirch H. 2008 Evidence for olfactory search in wandering
504 albatross, *Diomedea exulans*. *Proc. Natl. Acad. Sci. U. S. A.* **105**, 4576–4581.
505 (doi:10.1073/pnas.0709047105)
- 506 18. Bonadonna F, Villafañe ME, Bajzak C, Jouventin PJ. 2004 Recognition of burrow's olfactory
507 signature in blue petrels, *Halobaena caerulea*: an efficient discrimination mechanism in the
508 dark. *Anim. Behav.* **67**, 893–898.
- 509 19. Bang BG, Cobb S. 1968 The Size of the Olfactory Bulb in 108 Species of Birds. *Auk* **85**, 55–61.
510 (doi:10.2307/4083624)
- 511 20. Healy S, Guilford T. 1990 Olfactory-bulb size and nocturnality in birds. *Evolution (N. Y.)*. **44**,
512 339–346. (doi:10.1111/j.1558-5646.1990.tb05203.x)
- 513 21. Cardé RT, Willis MA. 2008 Navigational strategies used by insects to find distant, wind-
514 borne sources of odor. *J. Chem. Ecol.* **34**, 854–866. (doi:10.1007/s10886-008-9484-5)
- 515 22. Kennedy S, Marsh D. 1974 Pheromone-regulated anemotaxis in flying moths. *Science (80-.)*.
516 **184**, 999–1001. (doi:10.1126/science.184.4140.999)
- 517 23. Alerstam T, Bäckman J, Evans TJ. 2019 Optimal central place foraging flights in relation to
518 wind. *J. Ornithol.* (doi:10.1007/s10336-019-01677-4)
- 519 24. Bernard A, Rodrigues ASL, Cazalis V, Grémillet D. 2021 Toward a global strategy for
520 seabird tracking. *Conserv. Lett.* , 1–15. (doi:10.1111/conl.12804)
- 521 25. Halley E. 1686 An historical account of the Trade Winds, and Monsoons, observable in the
522 seas between and near the tropics, with an attempt to assign the physical cause of the said
523 winds. *Philos. Trans. R. Soc.* **16**, 153–168.
- 524 26. Haury LR, McGowan JA, Wiebe PH. 1978 Patterns and processes in the time-space scales of
525 plankton distributions.
- 526 27. Bertrand A, Grados D, Colas F, Bertrand S, Capet X, Chaigneau A, Vargas G, Mousseigne A,
527 Fablet R. 2014 Broad impacts of fine-scale dynamics on seascape structure from zooplankton
528 to seabirds. *Nat. Commun.* **5**, 5239. (doi:10.1038/ncomms6239)
- 529 28. Weimerskirch H. 2007 Are seabirds foraging for unpredictable resources? *Deep. Res. Part II*
530 *Top. Stud. Oceanogr.* **54**, 211–223. (doi:10.1016/j.dsr2.2006.11.013)

- 531 29. De Pascalis F *et al.* 2021 Searching on the edge: dynamic oceanographic features increase
532 foraging opportunities in a small pelagic seabird. *Mar. Ecol. Prog. Ser.* **668**, 121–132.
533 (doi:10.3354/meps13726)
- 534 30. Buckley NJ. 1997 Spatial-concentration effects and the importance of local enhancement in
535 the evolution of colonial breeding in seabirds. *Am. Nat.* **149**, 1091–1112.
- 536 31. Collet J, Patrick SC, Weimerskirch H. 2015 Albatrosses redirect flight towards vessels at the
537 limit of their visual range. *Mar. Ecol. Prog. Ser.* **526**, 199–205. (doi:10.3354/meps11233)
- 538 32. Nevitt GA. 2000 Olfactory foraging by Antarctic procellariiform seabirds: life at high
539 Reynolds numbers. *Biol. Bull.* **198**, 245–253.
- 540 33. Dias MP, Romero J, Granadeiro JP, Catry T, Pollet IL, Catry P. 2016 Distribution and at-sea
541 activity of a nocturnal seabird, the Bulwer's petrel *Bulweria bulwerii*, during the incubation
542 period. *Deep. Res. Part I Oceanogr. Res. Pap.* **113**, 49–56. (doi:10.1016/j.dsr.2016.03.006)
- 543 34. Bonnet-Lebrun AS *et al.* 2021 Seabird migration strategies: Flight budgets, diel activity
544 patterns and lunar influence. *in Prep.* **8**, 1–15. (doi:10.3389/fmars.2021.683071)
- 545 35. Waap S, Symondson WOC, Granadeiro JP, Alonso H, Serra-Goncalves C, Dias MP, Catry P.
546 2017 The diet of a nocturnal pelagic predator, the Bulwer's petrel, across the lunar cycle. *Sci.*
547 *Rep.* **7**, 1–10. (doi:10.1038/s41598-017-01312-3)
- 548 36. Calenge C. 2016 Analysis of Animal Movements in R : the adehabitatLT Package.
- 549 37. R Core Team. 2019 R: A language and environment for statistical computing. R Foundation
550 for Statistical Computing, Vienna, Austria.
- 551 38. Dell'Araccia G, Benhamou S, Dias MP, Granadeiro JP, Sudre J, Catry P, Bonadonna F. 2018
552 Flexible migratory choices of Cory's shearwaters are not driven by shifts in prevailing air
553 currents. *Sci. Rep.* **8**, 3376. (doi:10.1038/s41598-018-21608-2)
- 554 39. McClintock BT, Michelot T. 2018 momentuHMM: R package for generalized hidden Markov
555 models of animal movement. *Methods Ecol. Evol.* , 1–13. (doi:10.1111/2041-210X.12995)
- 556 40. Zucchini W, MacDonald IL. 2009 *Hidden Markov models for time series: an introduction using R.*
557 Chapman and Hall/CRC.
- 558 41. Patterson TA, Thomas L, Wilcox C, Ovaskainen O, Matthiopoulos J. 2008 State-space models
559 of individual animal movement. *Trends Ecol. Evol.* **23**, 87–94. (doi:10.1016/j.tree.2007.10.009)
- 560 42. Wood SN. 2006 *Generalized Additive Models: An Introduction with R.* Chapman and Hall/CRC.
- 561 43. Akaike H. 1998 A new look at the statistical model identification. In *Selected Papers of*
562 *Hirotsugu Akaike* (eds E Parzen, K Tanabe, G Kitagawa), pp. 215–222. New York, NY: Springer
563 New York. (doi:10.1007/978-1-4612-1694-0_16)

- 564 44. Holzbecher E. 2012 2D and 3D transport solutions (Gaussian Puffs and Plumes). In
565 *Environmental Modeling – Using MATLAB*, pp. 1–410. Berlin Heidelberg: Springer-Verlag.
566 (doi:10.1007/978-3-642-22042-5)
- 567 45. Oppel S *et al.* 2018 Spatial scales of marine conservation management for breeding seabirds.
568 *Mar. Policy* **98**, 37–46. (doi:10.1016/j.marpol.2018.08.024)
- 569 46. Shepherd TG. 2014 Atmospheric circulation as a source of uncertainty in climate change
570 projections. *Nat. Geosci.* **7**, 703–708.
- 571 47. Miranda PMA, Tomé R, Frois L, Nogueira M, Alves JMR, Prior V, Caldeira R, Dutra E. 2021
572 Speed-up of the Madeira tip jets in the ERA5 climate highlights the decadal variability of the
573 Atlantic subtropics. *Q. J. R. Meteorol. Soc.* **147**, 679–690. (doi:10.1002/qj.3940)
- 574
- 575

576 **Tables and figures**

577

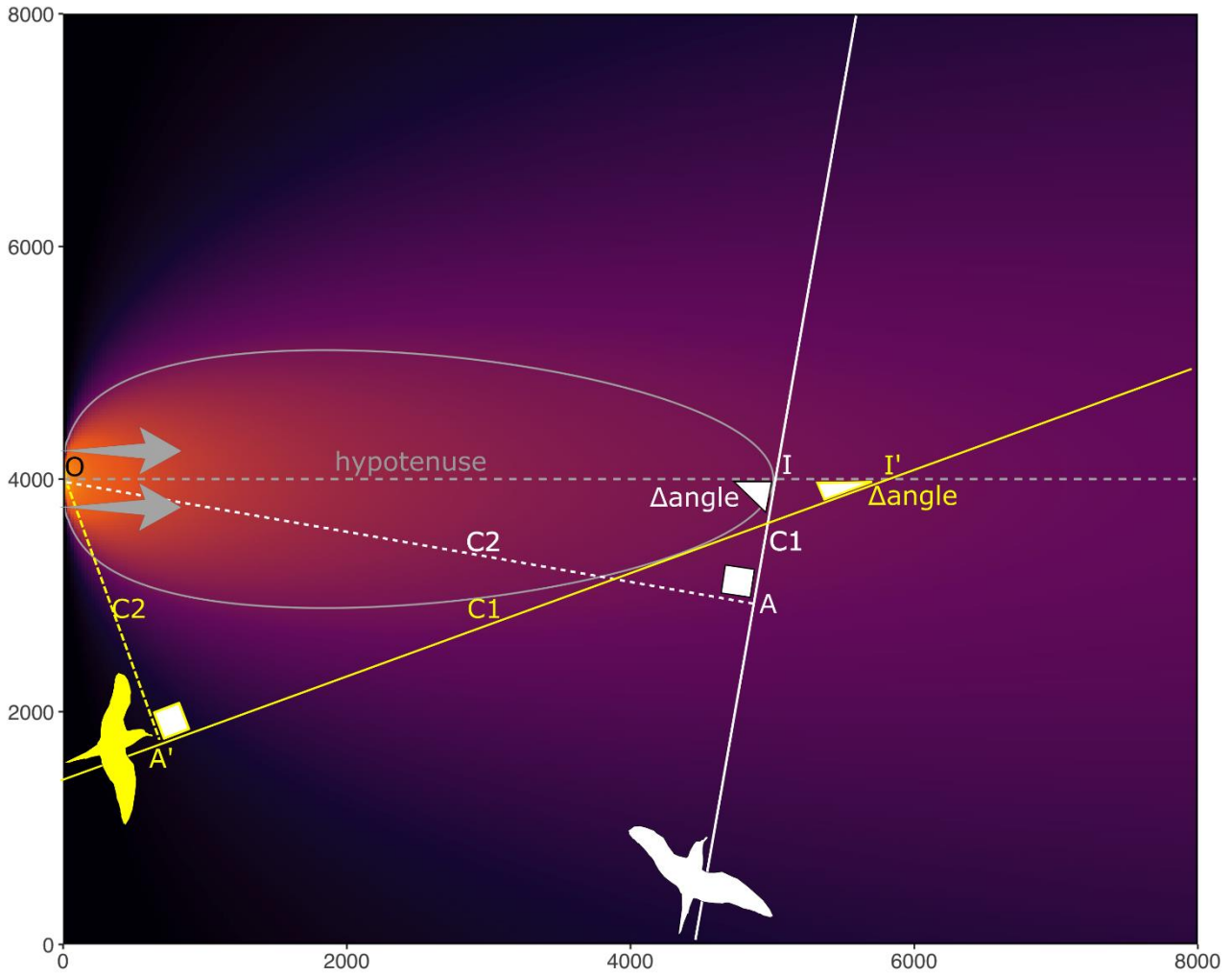
578 **Table 1.** The median and interquartile ranges of wind direction relative to the bird bearing
 579 ("Δangle") quantified for the different track sections and temporal resolution.

Trip Section (resolution)	Δangle, median	Δangle, 25%–75% interquartile range
Overall (3-min)	85.30°	65.96°–101.04°
In flight (3-min)	89.90°	77.94°–103.36°
Mixed (3-min)	85.85°	72.58°–100.39°
On water (3-min)	52.19°	22.99°– 92.45°
Day (3-min)	85.42°	65.54°–101.67°
Night (3-min)	84.80°	67.74°– 98.73°
Overall (1-h)	80.03°	58.92°– 96.35°
Transit (1-h)	79.04°	60.33°– 92.71°
Search (1-h)	81.16°	57.67°–100.01°
Day (1-h)	80.14°	57.91°– 97.33°
Night (1-h)	79.85°	61.36°– 94.31°
Nearby (1-h)	88.81°	76.95°–104.64°
Distant (1-h)	72.02°	49.07°– 88.81°

580

581

582

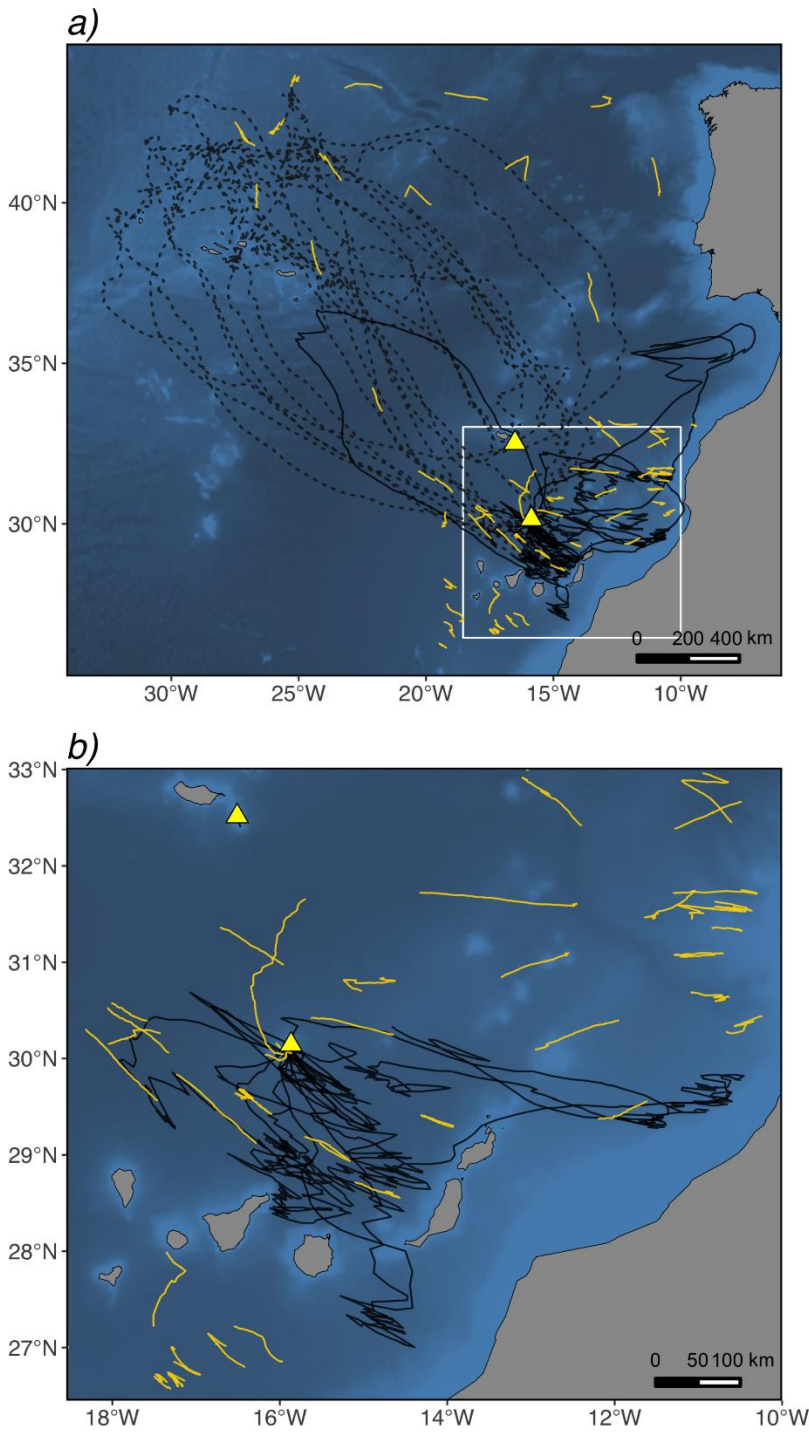


583

584 **Figure 1.** The smell detection contour generated by the "odor plume model". The constant and
 585 uniform wind is represented by the central arrows. The smell source is at "O". The x and y axes are
 586 expressed in meters. Two potential trajectories are depicted, with birds flying at two Δ angle
 587 values: 10° and 80° (coloured and white solid lines, respectively). Two right triangles are obtained,
 588 delimited by: the hypotenuse (OI' and OI for Δ angle of 10° and 80° respectively); the cathetus "C1"
 589 adjacent to Δ angle (A'I' and AI, adjacent to the Δ angle of 10° and 80°); and the cathetus "C2"
 590 opposite to Δ angle (OA' and OA). C2, calculated as $C2 = \text{hypotenuse} * \sin(\Delta\text{angle})$, is the "olfactory
 591 bandwidth", i.e. the maximum distance from the source at which a smell can be detected.

592

593

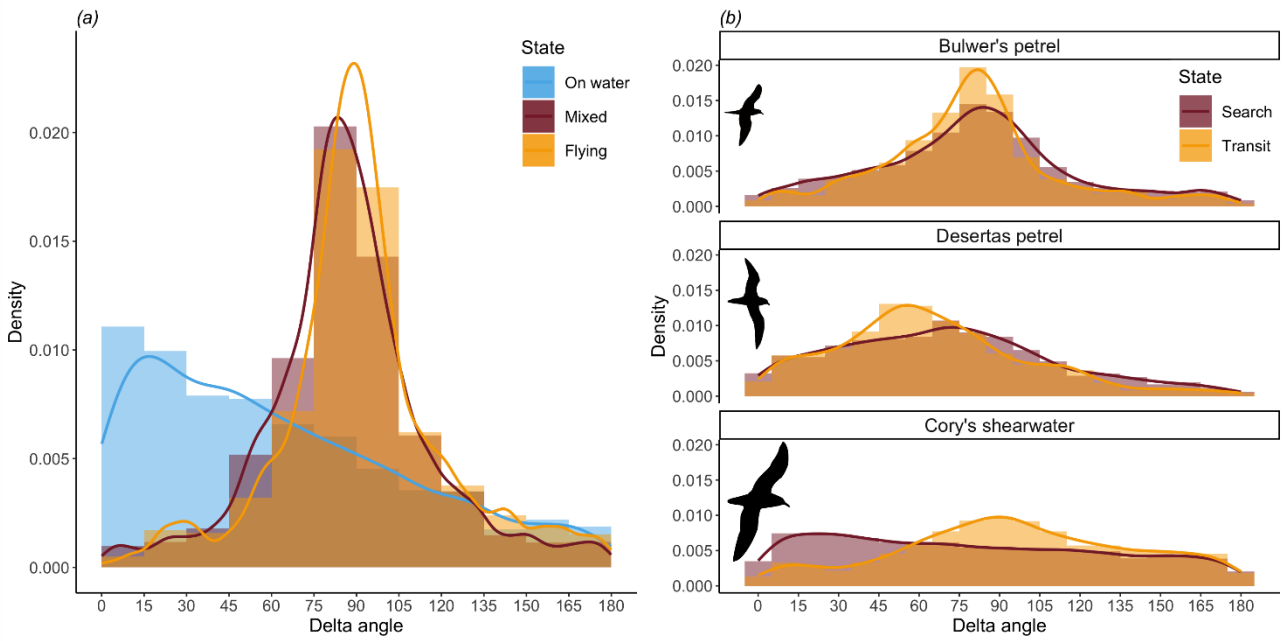


594

595 **Figure 2.** (a) All tracks, both at 3-min (in gold) and at 1-h resolution (in black) are depicted. The
 596 "distant" and "nearby" 1-h resolution trips are represented using dotted and solid lines,
 597 respectively. The inset map depicts the extent of panel (b) below. (b) A selection of 1-h and 3-min
 598 resolution tracks (in black and gold, respectively), highlighting the zig-zag flight performed by the
 599 petrels. The triangles indicate colony locations.

600

601

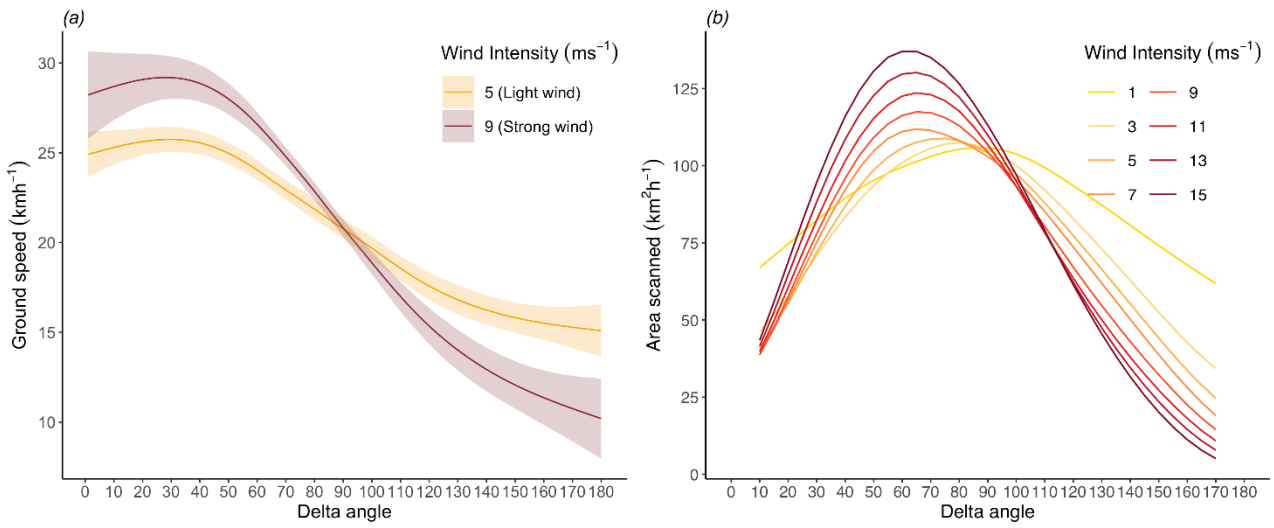


602

603 **Figure 3.** (a) Density curves of Δ angle used by the Bulwer's petrels along the 3 min resolution
 604 tracks. Different colors are used to represent the different behavioral states. (b) The Δ angle used by
 605 Bulwer's petrels along the 1-h resolution tracks during "search" and "transit" (in the top panel) is
 606 compared with that used by Desertas petrels (n = 25 tracks) and Cory's shearwaters (n = 103
 607 tracks).

608

609

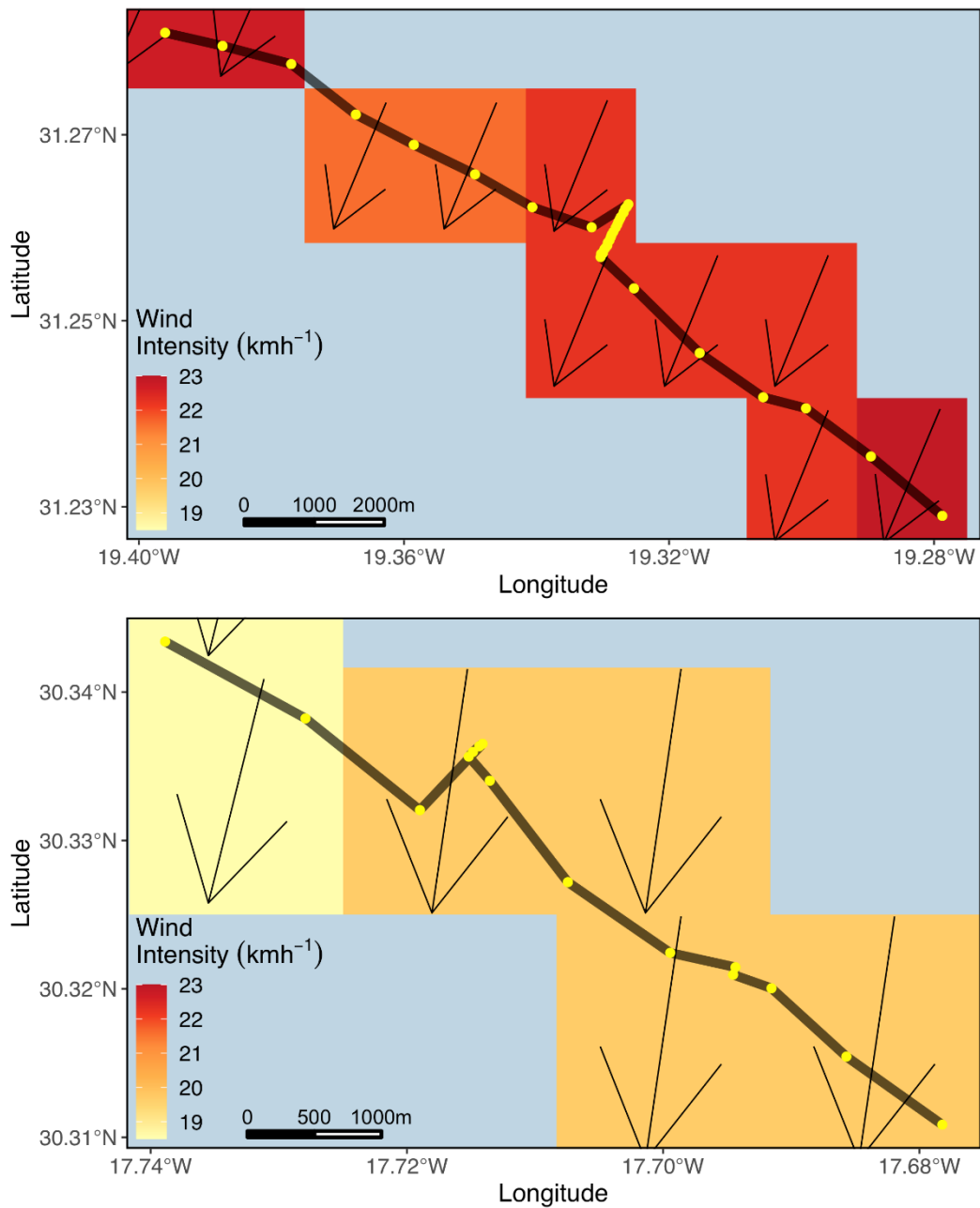


610

611 **Figure 4.** (a) GAMM "wind model", fitted to the transit segments of the 1-h resolution trips. The
 612 95% confidence interval is represented by the shaded areas. For visualization purpose, the
 613 predicted effect of Δ angle on ground speed (kmh⁻¹) was calculated for light (5 ms⁻¹) and strong (9
 614 ms⁻¹) winds. (b) The theoretical area olfactorily scanned (km² in 1 hour), as a function of wind
 615 Δ angle and wind intensity.

616

617



618

619 **Figure 5.** Two examples indicative of the occurrence of olfactory foraging along the 3-min
 620 resolution tracks. In both examples, the petrels fly crosswind, at night, moving from northwest to
 621 southeast. In two sections of the movement bouts (one per panel), the birds seem to: track the odor
 622 plume upwind for approximately 500 m; engage in foraging; sit on the surface of the water to
 623 process food (indicated by the sections in which the points are clustered together); finally, resume
 624 flying along the initial direction of movement. The arrows represent the real-time wind conditions
 625 experienced along the tracks, whereas the yellow points are the GPS locations.